Published in final edited form as:
Arterioscler Thromb Vasc Biol. 2012 March ; 32(3): 623–632. doi:10.1161/ATVBAHA.111.242180.

Dynamic immune cell accumulation during flow-induced atherogenesis in mouse carotid artery: An expanded flow cytometry method

Noah Alberts-Grill, B.A.[1,*], **Amir Rezvan, M.D.**[1,*], **Dong Ju Son, Ph.D.**[2], **Haiwei Qiu, B.S.**[2], **Chan Woo Kim, Ph.D.**[2], **Melissa L. Kemp, Ph.D.**[2], **Cornelia M. Weyand, MD, Ph.D.**[3], and **Hanjoong Jo, Ph.D.**[1,2,4,5]

[1]Emory University, School of Medicine, Cardiology Division

[2]Wallace H. Coulter Dept. of Biomedical Engineering, Georgia Institute of Technology and Emory University

[3]Stanford University, School of Medicine, Dept. of Immunology and Rheumatology

[4]Ewha Womans University, S. Korea.

Abstract

Objective—Inflammation plays a central role in atherosclerosis. However, the detailed changes in the composition and quantity of leukocytes in the arterial wall during atherogenesis are not fully understood due in part to the lack of suitable methods and animal models.

Methods and Results—We developed a 10-fluorochrome, 13-parameter flow cytometry method to quantitate 7 major leukocyte subsets in a single digested arterial wall sample. ApoE$^{-/-}$ mice underwent left carotid artery (LCA) partial ligation and fed high-fat diet for 4 to 28 days. Monocyte/macrophages, dendritic cells, granulocytes, NK cells, and CD4 T-cells significantly infiltrated the LCA as early as 4d. Monocyte/macrophages and dendritic cells decreased between 7d and 14d, while T-cell numbers remained steady. Leukocyte numbers peaked at 7d, preceding atheroma formation at 14d. B-cells entered LCA by 14d. Control right carotid and sham-ligated LCAs showed no significant infiltrates. PCR and ELISA arrays showed that expression of pro-inflammatory cytokines and chemokines peaked at 7 and 14-days post-ligation, respectively.

Conclusions—This is the first quantitative description of leukocyte number and composition over the life span of murine atherosclerosis. These results show that disturbed flow induces rapid and dynamic leukocyte accumulation in the arterial wall during the initiation and progression of atherosclerosis.

Keywords

Atherosclerosis; disturbed flow; leukocytes; flow cytometry; inflammation

[5]Correspondence: Ada Lee and Pete Correll Professor Coulter Department of Biomedical Engineering Department of Medicine, Division of Cardiology Georgia Institute of Technology and Emory University Woodruff Memorial Bldg, Rm 2005 Atlanta, GA 30322Phone: 404-712-9654 Fax: 404-727-9873 hjo@bme.gatech.edu.
[*]N.A.G. and A.R. contributed equally to this work.

c) Disclosures: None

INTRODUCTION

Atherosclerosis is an inflammatory disease driven in large part by immune cells that infiltrate into the arterial wall, leading to the development of lipid laden plaques[1-3]. The infiltration of immune cells and proliferation of smooth muscle cells (SMCs) into the artery wall plays a central role in atherogenesis. Macrophages, dendritic cells (DCs), and T-cells have all been shown to migrate into the intimal and adventitial regions of vessels in both the early and latter stages of atherogenesis in humans and in mice[4, 5]. Once present in the artery wall, each of these cell types contributes to atherogenesis in specific ways, such as presentation of atherogenic antigens to T-cells (DCs)[4, 6-8], foam cell formation by taking up lipids (macrophages, SMCs, DCs)[9], proinflammatory cytokine production (macrophages, T-cells)[3, 10-12], fibrous cap formation (SMCs), cytotoxicity (T-cells)[13-15], and extracellular matrix degradation (macrophages)[4].

Recently, we have shown that partial ligation of mouse carotid artery causes disturbed flow with characteristic low and oscillatory wall shear stress, leading to lipid-laden plaque development in apolipoprotein E-deficient ($ApoE^{-/-}$) mice fed a high-fat diet[16]. Using this model, we have shown that disturbed flow induces broad changes in the gene expression profile of endothelial cells (hours to days), including inter-cellular adhesion molecule 1 (ICAM-1) and vascular cell adhesion molecule 1 (VCAM-1) within 2 days[16, 17]. Impaired vascular relaxation response, another key aspect of endothelial dysfunction, occurs within 1 week via mechanisms involving eNOS uncoupling[18, 19], followed by the robust and homogenous formation of atheroma along the entire length of the common carotid artery within 2 weeks and features of advanced plaques such as intraplaque neovascular genesis by 4 weeks[16, 19].

While these results show a strong link between disturbed flow, inflammation, and atherosclerosis, the direct effect of disturbed flow on immune cell accumulation in the arterial wall during atherogenesis has not been established. However, in typical mouse models of diet-induced atherosclerosis, sufficient lesion growth typically takes more than two months in focal regions exposed to naturally disturbed flow[20]. This makes it difficult to conduct sensitive kinetic studies due to relatively small and non-homogenous lesion areas. In contrast, our flow-induced atherosclerosis model develops robust and homogenous atheroma along the entire length of the common carotid within two weeks, making it an ideal experimental platform to quantify and define relationships between immune cell accumulation and inflammation in the arterial wall.

Advances in multi-parameter flow cytometry allow for the surface phenotyping of a broad number of leukocyte cell types and their subsets using a single staining panel[21-23]. Flow cytometry has been previously used to track 1 to 4 different immune cell types in the vascular wall using 4 to 7 phenotypic markers[24-27]. Here we developed a 10-fluorochrome, 13-parameter flow cytometry method to phenotype and quantify seven major leukocyte subsets implicated in the pathogenesis of atherosclerosis. The flow cytometry data were validated by immunofluorescence staining studies and cytokine and chemokine gene expression profile studies were carried out to gain further functional insights into the mechanisms of leukocyte accumulation.

Here, we show that flow-disturbance causes rapid and dynamic immune cell accumulation in the arterial wall. Following flow disturbance, monocyte/macrophages and DCs rapidly infiltrate along with smaller numbers of T-cells, NK cells, and granulocytes within 7 days. Monocyte/macrophage and DC numbers then rapidly contract during plaque growth between 7 and 14 days post-ligation. The peak leukocyte accumulation was strongly correlated with IFNγ production.

METHODS

An expanded Methods section is available in Supplement.

Mice and Partial Carotid Ligation Surgery

ApoE$^{-/-}$ mice underwent partial ligation of the left carotid artery (LCA) as previously described, while untouched right carotid artery (RCA) and sham LCA were used as controls (Fig. 1A)[16, 28]. Following ligation, ApoE$^{-/-}$ mice were maintained on the Paigen's high-fat diet (HFD)[20] until sacrificed. These animal experiments were approved by the Institutional Animal Care and Use Committee of Emory University.

Ten-Channel, 13-Marker Flow Cytometric Analysis of Carotid Artery Leukocytes

LCA and RCA were excised and pooled (n=3) in collagenase digestion buffer, and digested as described[25]. Single cell suspensions were used for leukocyte phenotyping by flow cytometry (Fig. 1). In short, cells were stained with Fixable Live/Dead Yellow (LDY) stain to discriminate dead cells, followed by incubation with a cocktail containing monoclonal antibodies (mAb): CD45-biotin, CD8a-V450, CD11c-V450, CD4-FITC, Gr-1-FITC, CD49b-PE, NK1.1-PE, CD3e-PerCP-Cy5.5, CD11b-APC-Cy7, CD19-PE-Texas Red, F4/80-PE-Cy7, and MHCII-APC. Secondary staining of CD45-biotin was performed using streptavidin-conjugated Qdot 655. Immunofluorescence was detected using a LSR II flow cytometer, using AccuCount Ultra Rainbow Fluorescent Particles to determine absolute cell numbers. All flow analyses were performed using FlowJo analysis software (v5.0).

Immunostaining

Frozen sections (7 μm) of LCA and RCA[16], were stained with primary antibodies for CD45, α-smooth muscle actin (αSMA), CD11c, CD3, CD68, and CD11b and visualized with appropriate secondary antibodies. *In situ* apoptosis was measured by TUNEL assay and visualized by tetramethylrhodamine-dUTP (TMR) fluorescence.

PCR and Cytokine Bead Array ELISA Analysis of Chemokine and Cytokine Gene Expression

Total RNA obtained from LCA and RCA as described[16], were used for RT^2 Profiler PCR arrays. For Cytokine Bead Array (CBA) ELISAs, LCA and RCA were excised and stimulated in culture overnight as described[18]. Production of TNFα, IFNγ, IL-2, IL-4, and IL-5 was measured using the CBA ELISA kit according to manufacturer's protocol.

Partial Least Squares Regression (PLSR) Modeling Analysis

The relationship between immune cell accumulation dynamics and gene expression profiles were examined using the PLSR modeling method[29].

Statistical Analysis

Values are expressed as mean±SEM unless otherwise indicated. Pairwise comparisons were performed using one-way or two-way Student T-tests. Multiple comparisons of means were performed using 1-way ANOVA followed by Tukey's Multiple Comparison tests. Differences between groups were considered significant at P values below 0.05.

RESULTS

Development of a 10-fluorochrome, 13-parameter immunophenotyping study of leukocytes in the murine carotid artery

We developed a comprehensive, one-step flow cytometry method to accurately identify and quantify the composition of leukocyte sub-populations in nascent and established atherosclerotic lesions in the murine common carotid artery. Using a staining mixture containing 12 specific monoclonal antibodies conjugated to 10 different fluorochromes and a special gating strategy, we differentiated whole leukocyte populations into CD4 and CD8 T-cells, B-cells, monocyte/macrophages, DCs, granulocytes, and NK cells using mouse carotid artery (Fig. 1D). Flow cytometry antibodies were validated on enzyme-digested splenocytes and population gates were set according to fluorescence-minus-one controls (Supplemental Fig. I). The immunophenotyping method showed expected results in blood leukocytes and splenocytes (Supplemental Fig. II), and stains of digested aorta preparations yielded similar results to previous studies (Supplemental Fig. III)[23, 25].

Flow disturbance causes rapid and dynamic accumulation of leukocytes into the arterial wall in a time-dependent manner

Using the 13-parameter immunotyping method, we then examined leukocyte number and composition in arterial wall during the development of atherosclerosis. Following partial ligation surgery and HFD, flow-disturbed left common carotid artery (LCA) and control right carotid arteries (RCA) obtained at 4, 7, 14, 21, and 28 days post-ligation were enzymatically digested and analyzed by flow cytometry (Fig. 1).

As shown in Figure 2A, flow-disturbance caused a dynamic increase in leukocyte numbers in LCA in a time-dependent manner. Approximately 500 leukocytes were found per LCA as early as 4 days post-ligation. Leukocyte numbers peaked in LCA at ~9,200 cells at 7 days, and surprisingly, contracted to ~2,900 cells by 14 day, maintaining similar numbers in the vessel wall through 28 days post-ligation (Supplemental Table I). In contrast, leukocytes did not significantly infiltrate into unligated RCA or sham-operated LCA (Fig. 2B-C). To determine whether the decline in leukocyte numbers from day 7 to day 14 was due to cell recovery artifacts during extraction, we quantified the number of dead (LDY^+) and non-singlet, or “clumped”, $CD45^+$ cells over the time course (Supplemental Fig. IV). Leukocyte viability did not change over the time course, although significantly increased numbers of clumped $CD45^+$ cells were seen at 7 and 21 days post-ligation (Supplemental Fig. IV). These results indicate that the decline in arterial leukocytes is not likely due to an extraction artifact.

To further validate the flow cytometry data for dynamic leukocyte infiltration into LCA, LCA and RCA were stained with CD45 antibody. As additional controls, we used markers of SMC (αSMA) and apoptosis (TUNEL). Intense CD45 staining in LCA was observed in the intimal lesion at 7, 14, or 21 days post-ligation, as well as in the media and adventitia (especially at 7 days) (Fig. 2D). In contrast, CD45 staining was not observed in RCA sections in either 7 or 21 day samples as well as in sham-operated LCA and RCA. Interestingly, intimal αSMA staining was not apparent at day 7, but intense staining was found throughout the intima at day 14, which then regressed to a more localized peri-luminal pattern by day 21 (Fig. 2E). Further, a small number of apoptotic cells appear at day 7, which significantly and transiently increased at day 14, followed by a decrease by day 21 (Fig. 2F). Semi-quantitative analysis of the staining data supports the qualitative observations. Taken together, these results suggest that the lesion growth from day 7 to day 14 is largely accounted for by SMC accumulation along with decreased but sustained presence of leukocytes (Fig. 2D-F).

Disturbed flow induces dynamic accumulation of innate cells, T- and B-cells in LCA

The flow cytometry data shown in Figure 2A was further analyzed to quantify dynamic changes in specific innate and adaptive immune cell populations. Total $CD45^+$ leukocytes were gated into B-cells, T-cells, DCs, monocyte/macrophages, NK cells, and granulocytes (Fig. 1D). The time course data showed that flow disturbance induced rapid infiltration of all four innate cell types tested (DC, monocyte/macrophage, NK cells, granulocytes) within 4 days and transiently peaking at 7 days (Fig. 3A; Supplemental Table I). The number of DCs and monocyte/macrophages in LCA significantly contracted between 7 and 14 days post-ligation, but remained steady afterwards. NK cell numbers steadily declined from day 7 to day 28 post-ligation, while granulocytes showed a non-significant, bi-phasic pattern over the time course with peaks at 7 and 28 days. In contrast, B-cells did not significantly enter the arterial wall until day 14 post-ligation, and peaked by day 21 (Fig. 3A). Disturbed flow induced the infiltration of a surprisingly small, but statistically significant number of T-cells as early as day 4, which significantly increased by day 7 and remained at ~180 cells between day 14 and 28 post-ligation (Fig. 3A). Total infiltrating T-cells were further divided into CD4 and CD8 T-cells (Fig. 3B). CD4 cells were found to infiltrate into LCA as early as 4 days, peaking at 7 days and remaining high without a significant contraction for the duration of the time course. In contrast, CD8 cells were also found to infiltrate into LCA only by day 7 and remained unchanged over the time course, while maintaining ~ 2:1 ratio (CD4/CD8) (Fig. 3B).

We next performed combined compositional analyses of leukocytes in the carotid wall by calculating the percentage of each immune cell subtype out of total leukocyte numbers over the time course (Fig. 3C). As expected, monocyte/macrophages were the dominant immune cell in the flow-disturbed LCA, followed by DCs. Interestingly, T-cell and B-cell percentages appear to increase as the atherosclerotic lesion develops (14 to 28 days) compared to early lesions (4 to 7 days post-ligation), as did NK cells.

Disturbed flow induces intimal accumulations of macrophages, DCs, and CD4 T-cells in LCA

To validate the quantitative flow cytometry data, we performed immunofluorescence staining studies with antibodies specific to macrophage/foam cells, DCs, and T-cells using frozen LCA and RCA cross-sections from ligated $ApoE^{-/-}$ mice. Both 7 and 21 day post-ligation lesions stained intensely for the macrophage/foam cell marker CD68 and myeloid cell marker CD11b both in the intima and adventitia (Fig. 4A-B). Within the intima, CD68 and CD11b staining was localized to nuclei-dense regions of the lesion, especially at 3 weeks (Fig. 4B). The extensive intimal and adventitial CD68 staining in both 7 and 21 day lesions suggests that rapid foam cell differentiation occurs in leukocytes accumulating in the flow-disturbed LCA. In contrast to CD68 and CD11b staining, CD11c (DC) staining occurred mostly in intimal lesions but not in adventitia (Fig. 4). Similar to CD11c staining, T-cell infiltration (CD3) was also restricted to the intima in 21 day lesion, although it was also found in the media and adventitia at day 7. Since the animals were fed HFD, occasional $CD11b^+$ and $CD68^+$ cells were found in the adventitia of RCAs (Fig. 4A-B). Isotype control stains for all antibodies used showed negative staining in carotid intima, media, and adventitia (Fig. 4C). Collectively, these results support the flow cytometry results.

Disturbed flow induces dynamic changes in cytokine and chemokine gene expression in LCA, and show Th1 T-cell mediated inflammatory pathology

To determine the effect of disturbed flow on cytokine and chemokine production in mouse carotid wall, we carried out RT^2 Profiler PCR arrays (SA Biosciences) on RNA from LCA and RCA taken at 4, 7, or 14 days post-ligation in $ApoE^{-/-}$ mice. In total, the expression levels of 89 genes, including 5 house-keeping genes were analyzed per sample. As shown in

the heat map (Fig. 5A) and volcano plots (Supplemental Fig. V), we found no significantly altered gene expression (≥3-fold) in LCA at 4 days, but 53 genes were significantly upregulated at 7 and 14 days (Supplemental Table II). Interestingly, however, the PCR array failed to detect interferon γ *(Ifng)*, a well-known, critical atherogenic cytokine (Fig. 5A), which may have been due to a poor primer set. Therefore, we retested the same RNA samples using a different primer sequence set, and found that *Ifng* expression was significantly increased in LCA at 7 days, but not at 4 or 14 days post-ligation (Fig. 5B).

To further determine IFNγ production by cells in flow-disturbed lesions, cytokine expression was induced *ex vivo* by culturing LCA and RCA overnight in the presence of 12-O-tetradecanoylphorbol-13-acetate (TPA) and ionomycin. Production of IFNγ, tumor necrosis factor α (TNFα), interleukin 2 (IL-2), interleukin 4 (IL-4), and interleukin 5 (IL-5) protein expression was assessed in culture supernatants by cytokine bead array ELISA. IFNγ, IL-2 and TNFα production was robustly increased in LCA, but not in RCA, obtained from 7 day post-ligated mice (Fig. 5C). IL-5 was increased as well in LCA, while IL-4 levels were not detected in LCA or RCA by the ELISA (Fig. 5C). These results suggest that disturbed flow induces Th1-skewed inflammation.

To further examine the Th1-skewed response, we performed additional qPCR for Th-lineage specific transcription factors, *Tbx21* (for Th1), *Gata3* (for Th2), *Rorc* (for Th17) and *Foxp3* (for Treg) using the same samples used in Figure 5A. We found that *Tbx21* was upregulated by 7 and 14 days, while *Gata3* did not change in LCA until 14 days post-ligation (Fig. 5D). These results are consistent with the *Ifng* qPCR result and the ELISA data (Fig. 5B-C), confirming the presence of a Th1-skewed immune response in the flow-disturbed LCA. In addition, *Rorc* and *Foxp3* transcription factors were upregulated at 7 and 14 days, indicating the presence of Th17 and Treg cells in LCA as well.

Vascular inflammation kinetics correspond with immune cell infiltration kinetics *in vivo* – a modeling study

PLSR analysis was used to model the relationship between changes in cytokine/cytokine receptor gene expression and leukocyte accumulation dynamics in the arterial wall following exposure to disturbed flow. The optimized model consisted of 4 statistically significant components with a R^2Y =0.943 and Q^2 =0.757, suggesting a strong fit between observed changes in gene expression and immune cell numbers. Days 7 and 14 form distinct clusters on the scores plot indicating a separation of gene expression trends between the two days of collection (Supplemental Fig. VI). From the scores plot, the positive PC2 direction roughly relates with information contained in day 7 samples, and the positive PC1 direction with information contained in day 14 samples.

Similarly, a loadings scatter plot maps the relative importance, or weight contribution, of X or Y-block variables to a principal component. There is a separation between most X- and Y-variables, save for IFNγ, which shows a strong correlation with the number of immune cells recruited into LCA by day 7 post-ligation (Supplemental Fig. VII). In contrast, the strong relation of the remaining genes to day 14 LCA samples suggests that the inflammatory cytokine response increases after immune cell recruitment, corresponding with SMC migration into the carotid intima and plaque growth (Fig. 2E).

DISCUSSION

The involvement of immune cells in atherogenesis has been well-established[3]. While multi-parameter or multiplex flow cytometry methods that are capable of analyzing up to 15 different markers have been used[21, 23, 30-33], they have not been applied to study immune cell kinetics in atherosclerosis to our knowledge. Multi-parameter flow cytometry studies in

the atherosclerosis field have typically used up to 4-7 surface phenotype markers despite the discovery of increasingly more complex subsets of macrophages and DCs important to atherogenesis[7, 25, 34-39]. To overcome this issue, we developed a robust 13-parameter, 10-fluorochrome flow cytometry method to analyze the kinetics of 7 distinct leukocyte types in atherosclerotic lesions.

We applied this flow cytometry method to lesion samples from our disturbed flow model of atherosclerosis. The major advantage of this murine model is that it induces atherogenesis rapidly and reproducibly along the entire length of LCA, beginning with a healthy disease-free artery and leading to a fully-developed atheroma in only a few weeks. This allowed us to track week-to-week and even day-to-day changes in immune cell populations within the developing atherosclerotic lesion. The flow cytometry findings in LCA and RCA were validated by immunostaining with CD45, CD11b, CD11c, CD3, and CD68 (Fig. 2 and 4). CD45, CD11b, and CD68 stains show that some vascular wall leukocytes detected by the flow cytometry method likely reside within the adventitia or media and do not necessarily represent intimal plaque leukocytes. In contrast to flow-disturbed LCA, athero-resistant RCA and sham-operated LCA contained only a few resident leukocytes and did not show sustained immune cell accumulations throughout the study.

The most dominant feature of our immune cell kinetic results was a surge of leukocyte numbers at 7 days post-ligation, followed by substantial contraction of innate leukocytes at day 14, primarily comprised of monocyte/macrophages and DCs (Fig. 3, Supplemental Table I). This appears to be in conflict with previous studies that reported progressive leukocyte accumulation, especially of monocyte-derived macrophages and DCs, in the arterial wall during atherogenesis[3, 25, 40, 41]. Immunostaining for SMCs (αSMA) and *in situ* apoptosis show heavy SMC migration and increased cell death in intimal plaques, corresponding with decreased CD45 staining at 14 and 21 days post-ligation (Fig. 2D-F). Together, the data suggest that leukocyte death, along with fibrous cap formation, account for some of the observed leukocyte regression. However, cell egress early during lesion initiation cannot be ruled out as a potential mechanism for macrophage/DC loss in our model, which is interesting since efflux of monocyte-derived cells has been shown to be primarily associated with lesion regression[40, 41]. Another limitation in comparing these findings to previous work is that in our model, flow disturbance induces an accelerated atherogenesis with proportionately low numbers of T-cells and increased numbers of monocyte/macrophages, DCs, NK cells, and granulocytes compared to previous findings in aorta (Supplemental Fig. III)[25]. Whether this is due to the disturbed flow-model used or the arteries examined in this study requires further research, although neutrophil margination and transmigration has been previously reported in atherosclerosis of the carotid bifurcation[42].

The surge in leukocyte accumulation correlates with the initiation of inflammatory cytokine and chemokine expression in our PCR Array studies (Fig. 5, Supplemental Table II), especially pro-atherogenic cytokines TNFα and IFNγ, which have been shown to play central, necessary roles in atherogenesis[3, 10, 43]. These findings suggest that the early surge in immune cells contributes directly to the increased inflammation and rapid plaque growth seen in our model, a conjecture supported by the PLSR modeling analysis, which shows that the immune cell kinetics measured in our study correlate well with changes in inflammatory gene expression (Supplemental Fig. VI and VII). In particular, the analysis indicated a predominant role for IFNγ in immune cell-mediated inflammatory pathology within the flow-disturbed region, leading to a cascade of subsequent pro-inflammatory gene upregulation and atheromatous plaque development by day 14.

Additionally, atherosclerosis-associated chemokines for monocytes (*Ccl2*, *Cxcl2*, *Ccl7*), DCs (*Cx3cl1*, *Ccl19*, *Ccl9*), T-cells (*Ccl5*, *Cxcl9*), neutrophils (*Ccl3*, *Ccl24*), NK cells (*Cxcl10*, *Ccl4*), and B-cells (*Cxcl12*, *Ccl19*) were detected in flow-disturbed LCA (Supplemental Table II), further linking disturbed flow to established mechanisms of leukocyte trafficking in atherosclerosis[3]. These results correspond with recent whole genome profiles of human coronary and carotid artery plaques[44]. We also found significantly increased levels of the Th1 T-cell-specific transcription factor T-bet (*Tbx21*) at day 7 post-ligation, which were sustained through day 14 (Fig. 5), which correlate with the sustained, albeit low, numbers of CD4 and CD8 T-cells seen in LCA at 14 days post-ligation and beyond (Fig 3B). The presence of T-bet expression in LCA suggests that flow-disturbance induces the Th1-skewed adaptive immune response typical of atherosclerosis[45]. This was confirmed by ELISA array assays, which showed a distinct Th1 cytokine signature in flow-disturbed LCA stimulated *ex vivo*. Our model also showed the presence of Th17 T-cells (*Rorc*) and Tregs (*Foxp3*) in the plaque along with slight increases in *Il17a* and *Il10* gene expression (Fig. 5) as previously reported in humans and mice[11, 12, 34, 46].

Flow cytometry provides a more accurate and unbiased method to quantify arterial immune cells than previously used histological approaches. However, the use of enzymatic tissue digestion and homogenization to extract vascular leukocytes may induce cell death (Supplemental Fig. IV) or other enzymatic extraction-dependent artifacts that may affect the flow cytometry results systematically or in a sub-population-dependent manner. Furthermore, low leukocyte counts in some of our samples (i.e., greater (GC) and lesser (LC) curvature of the aortic arch and LCA at 4 days post-ligation) could undermine the statistical accuracy of our quantitative and phenotypic percentage data (Fig. 2A, 3, Supplemental Fig. III). As such, our flow cytometry results need to be interpreted with appropriate caution.

Our studies establish partial carotid ligation as an effective animal model to study the inflammatory pathogenesis of atherosclerosis. We provide a comprehensive quantitative description of infiltrating leukocyte number and composition over the entire life span of an atherosclerotic lesion. We show that rather than being progressive, leukocyte accumulation in the flow-disturbed vascular lesion is dynamic, and that peak leukocyte accumulation immediately precedes major plaque development.

Supplementary Material

Refer to Web version on PubMed Central for supplementary material.

Acknowledgments

a) Acknowledgements: None

b) Sources of Funding: Work supported by funding from NIH grants HL095070, HL70531, HHSN268201000043C, and a World Class University Project in Korea (R31-2008-000-10010-0) to HJ.

REFERENCES

1. Hansson GK. Inflammation, atherosclerosis, and coronary artery disease. N Engl J Med. 2005; 352:1685–1695. [PubMed: 15843671]
2. Libby P. Inflammation in atherosclerosis. Nature. 2002; 420:868–874. [PubMed: 12490960]
3. Galkina E, Ley K. Immune and inflammatory mechanisms of atherosclerosis (*). Annu Rev Immunol. 2009; 27:165–197. [PubMed: 19302038]
4. Hansson GK, Hermansson A. The immune system in atherosclerosis. Nat Immunol. 2011; 12:204–212. [PubMed: 21321594]

5. Hansson GK, Robertson AK, Soderberg-Naucler C. Inflammation and atherosclerosis. Annu Rev Pathol. 2006; 1:297–329. [PubMed: 18039117]
6. Hermansson A, Ketelhuth DF, Strodthoff D, Wurm M, Hansson EM, Nicoletti A, Paulsson-Berne G, Hansson GK. Inhibition of T cell response to native low-density lipoprotein reduces atherosclerosis. J Exp Med. 2010; 207:1081–1093. [PubMed: 20439543]
7. Hjerpe C, Johansson D, Hermansson A, Hansson GK, Zhou X. Dendritic cells pulsed with malondialdehyde modified low density lipoprotein aggravate atherosclerosis in ApoE(-/-) mice. Atherosclerosis. 2010; 209:436–441. [PubMed: 19897195]
8. Niessner A, Weyand CM. Dendritic cells in atherosclerotic disease. Clin Immunol. 2010; 134:25–32. [PubMed: 19520615]
9. Paulson KE, Zhu SN, Chen M, Nurmohamed S, Jongstra-Bilen J, Cybulsky MI. Resident intimal dendritic cells accumulate lipid and contribute to the initiation of atherosclerosis. Circ Res. 2010; 106:383–390. [PubMed: 19893012]
10. McLaren JE, Ramji DP. Interferon gamma: A master regulator of atherosclerosis. Cytokine Growth Factor Rev. 2009; 20:125–135. [PubMed: 19041276]
11. Erbel C, Chen L, Bea F, Wangler S, Celik S, Lasitschka F, Wang Y, Bockler D, Katus HA, Dengler TJ. Inhibition of IL-17a attenuates atherosclerotic lesion development in ApoE-deficient mice. J Immunol. 2009; 183:8167–8175. [PubMed: 20007582]
12. Eid RE, Rao DA, Zhou J, Lo SF, Ranjbaran H, Gallo A, Sokol SI, Pfau S, Pober JS, Tellides G. Interleukin-17 and interferon-gamma are produced concomitantly by human coronary artery-infiltrating T cells and act synergistically on vascular smooth muscle cells. Circulation. 2009; 119:1424–1432. [PubMed: 19255340]
13. Nakajima T, Goek O, Zhang X, Kopecky SL, Frye RL, Goronzy JJ, Weyand CM. De novo expression of killer immunoglobulin-like receptors and signaling proteins regulates the cytotoxic function of CD4 T cells in acute coronary syndromes. Circ Res. 2003; 93:106–113. [PubMed: 12816883]
14. Pryshchep S, Sato K, Goronzy JJ, Weyand CM. T cell recognition and killing of vascular smooth muscle cells in acute coronary syndrome. Circ Res. 2006; 98:1168–1176. [PubMed: 16601227]
15. Nakajima T, Schulte S, Warrington KJ, Kopecky SL, Frye RL, Goronzy JJ, Weyand CM. T-cell-mediated lysis of endothelial cells in acute coronary syndromes. Circulation. 2002; 105:570–575. [PubMed: 11827921]
16. Nam D, Ni CW, Rezvan A, Suo J, Budzyn K, Llanos A, Harrison D, Giddens D, Jo H. Partial carotid ligation is a model of acutely induced disturbed flow, leading to rapid endothelial dysfunction and atherosclerosis. Am J Physiol Heart Circ Physiol. 2009; 297:H1535–1543. [PubMed: 19684185]
17. Ni CW, Qiu H, Rezvan A, Kwon K, Nam D, Son DJ, Visvader JE, Jo H. Discovery of novel mechanosensitive genes in vivo using mouse carotid artery endothelium exposed to disturbed flow. Blood. 2010; 116:e66–73. [PubMed: 20551377]
18. Li L, Chen W, Rezvan A, Jo H, Harrison DG. Tetrahydrobiopterin deficiency and nitric oxide synthase uncoupling contribute to atherosclerosis induced by disturbed flow. Arterioscler Thromb Vasc Biol. 2011; 31:1547–1554. [PubMed: 21512164]
19. Li L, Rezvan A, Salerno JC, Husain A, Kwon K, Jo H, Harrison DG, Chen W. GTP cyclohydrolase I phosphorylation and interaction with GTP cyclohydrolase feedback regulatory protein provide novel regulation of endothelial tetrahydrobiopterin and nitric oxide. Circ Res. 2010; 106:328–336. [PubMed: 19926872]
20. Paigen B, Morrow A, Holmes PA, Mitchell D, Williams RA. Quantitative assessment of atherosclerotic lesions in mice. Atherosclerosis. 1987; 68:231–240. [PubMed: 3426656]
21. Chattopadhyay PK, Price DA, Harper TF, Betts MR, Yu J, Gostick E, Perfetto SP, Goepfert P, Koup RA, De Rosa SC, Bruchez MP, Roederer M. Quantum dot semiconductor nanocrystals for immunophenotyping by polychromatic flow cytometry. Nat Med. 2006; 12:972–977. [PubMed: 16862156]
22. Perfetto SP, Ambrozak D, Nguyen R, Chattopadhyay P, Roederer M. Quality assurance for polychromatic flow cytometry. Nat Protoc. 2006; 1:1522–1530. [PubMed: 17406444]

23. Frischmann U, Muller W. Nine fluorescence parameter analysis on a four-color fluorescence activated flow cytometer. Cytometry A. 2006; 69:124–126. [PubMed: 16496423]
24. Swirski FK, Libby P, Aikawa E, Alcaide P, Luscinskas FW, Weissleder R, Pittet MJ. Ly-6C-hi monocytes dominate hypercholesterolemia-associated monocytosis and give rise to macrophages in atheromata. J Clin Invest. 2007; 117:195–205. [PubMed: 17200719]
25. Galkina E, Kadl A, Sanders J, Varughese D, Sarembock IJ, Ley K. Lymphocyte recruitment into the aortic wall before and during development of atherosclerosis is partially L-selectin dependent. J Exp Med. 2006; 203:1273–1282. [PubMed: 16682495]
26. Zhou J, Tang PC, Qin L, Gayed PM, Li W, Skokos EA, Kyriakides TR, Pober JS, Tellides G. CXCR3-dependent accumulation and activation of perivascular macrophages is necessary for homeostatic arterial remodeling to hemodynamic stresses. J Exp Med. 2010; 207:1951–1966. [PubMed: 20733031]
27. Smith E, Prasad KM, Butcher M, Dobrian A, Kolls JK, Ley K, Galkina E. Blockade of interleukin-17a results in reduced atherosclerosis in apolipoprotein E-deficient mice. Circulation. 2010; 121:1746–1755. [PubMed: 20368519]
28. Nam D, Ni CW, Rezvan A, Suo J, Budzyn K, Llanos A, Harrison DG, Giddens DP, Jo H. A model of disturbed flow-induced atherosclerosis in mouse carotid artery by partial ligation and a simple method of RNA isolation from carotid endothelium. J Vis Exp. 2010
29. Rivet CA, Hill AS, Lu H, Kemp ML. Predicting cytotoxic T-cell age from multivariate analysis of static and dynamic biomarkers. Mol Cell Proteomics. 2011; 10 M110 003921.
30. Wood BL. Ten-color immunophenotyping of hematopoietic cells. Curr Protoc Cytom. 2005 Chapter 6:Unit6 21.
31. Song K, Bolton DL, Wei CJ, Wilson RL, Camp JV, Bao S, Mattapallil JJ, Herzenberg LA, Andrews CA, Sadoff JC, Goudsmit J, Pau MG, Seder RA, Kozlowski PA, Nabel GJ, Roederer M, Rao SS. Genetic immunization in the lung induces potent local and systemic immune responses. Proc Natl Acad Sci U S A. 2010; 107:22213–22218. [PubMed: 21135247]
32. Hotson AN, Hardy JW, Hale MB, Contag CH, Nolan GP. The T cell STAT signaling network is reprogrammed within hours of bacteremia via secondary signals. J Immunol. 2009; 182:7558–7568. [PubMed: 19494279]
33. Yamamoto T, Price DA, Casazza JP, Ferrari G, Nason M, Chattopadhyay PK, Roederer M, Gostick E, Katsikis PD, Douek DC, Haubrich R, Petrovas C, Koup RA. Surface expression patterns of negative regulatory molecules identify determinants of virus-specific CD8+ T-cell exhaustion in HIV infection. Blood. 2011; 117:4805–4815. [PubMed: 21398582]
34. Gotsman I, Grabie N, Gupta R, Dacosta R, MacConmara M, Lederer J, Sukhova G, Witztum JL, Sharpe AH, Lichtman AH. Impaired regulatory T-cell response and enhanced atherosclerosis in the absence of inducible costimulatory molecule. Circulation. 2006; 114:2047–2055. [PubMed: 17060381]
35. Tacke F, Alvarez D, Kaplan TJ, Jakubzick C, Spanbroek R, Llodra J, Garin A, Liu J, Mack M, van Rooijen N, Lira SA, Habenicht AJ, Randolph GJ. Monocyte subsets differentially employ CCR2, CCR5, and CX3CR1 to accumulate within atherosclerotic plaques. J Clin Invest. 2007; 117:185–194. [PubMed: 17200718]
36. Combadiere C, Potteaux S, Rodero M, Simon T, Pezard A, Esposito B, Merval R, Proudfoot A, Tedgui A, Mallat Z. Combined inhibition of CCL2, CX3CR1, and CCR5 abrogates Ly-6C-(hi) and Ly-6C-(lo) monocytosis and almost abolishes atherosclerosis in hypercholesterolemic mice. Circulation. 2008; 117:1649–1657. [PubMed: 18347211]
37. Galkina E, Harry BL, Ludwig A, Liehn EA, Sanders JM, Bruce A, Weber C, Ley K. CXCR6 promotes atherosclerosis by supporting T-cell homing, interferon-gamma production, and macrophage accumulation in the aortic wall. Circulation. 2007; 116:1801–1811. [PubMed: 17909108]
38. Guzik TJ, Hoch NE, Brown KA, McCann LA, Rahman A, Dikalov S, Goronzy J, Weyand C, Harrison DG. Role of the T cell in the genesis of angiotensin II induced hypertension and vascular dysfunction. J Exp Med. 2007; 204:2449–2460. [PubMed: 17875676]
39. Bu DX, Tarrio M, Maganto-Garcia E, Stavrakis G, Tajima G, Lederer J, Jarolim P, Freeman GJ, Sharpe AH, Lichtman AH. Impairment of the programmed cell death-1 pathway increases

atherosclerotic lesion development and inflammation. Arterioscler Thromb Vasc Biol. 2011; 31:1100–1107. [PubMed: 21393583]

40. Randolph GJ. Emigration of monocyte-derived cells to lymph nodes during resolution of inflammation and its failure in atherosclerosis. Curr Opin Lipidol. 2008; 19:462–468. [PubMed: 18769227]
41. Potteaux S, Gautier EL, Hutchison SB, van Rooijen N, Rader DJ, Thomas MJ, Sorci-Thomas MG, Randolph GJ. Suppressed monocyte recruitment drives macrophage removal from atherosclerotic plaques of ApoE-/- mice during disease regression. J Clin Invest. 2011; 121:2025–2036. [PubMed: 21505265]
42. Drechsler M, Megens RT, van Zandvoort M, Weber C, Soehnlein O. Hyperlipidemia-triggered neutrophilia promotes early atherosclerosis. Circulation. 2010; 122:1837–1845. [PubMed: 20956207]
43. Tedgui A, Mallat Z. Cytokines in atherosclerosis: Pathogenic and regulatory pathways. Physiol Rev. 2006; 86:515–581. [PubMed: 16601268]
44. Cagnin S, Biscuola M, Patuzzo C, Trabetti E, Pasquali A, Laveder P, Faggian G, Iafrancesco M, Mazzucco A, Pignatti PF, Lanfranchi G. Reconstruction and functional analysis of altered molecular pathways in human atherosclerotic arteries. BMC Genomics. 2009; 10:13. [PubMed: 19134193]
45. Schulte S, Sukhova GK, Libby P. Genetically programmed biases in Th1 and Th2 immune responses modulate atherogenesis. Am J Pathol. 2008; 172:1500–1508. [PubMed: 18467709]
46. Gotsman I, Gupta R, Lichtman AH. The influence of the regulatory T lymphocytes on atherosclerosis. Arterioscler Thromb Vasc Biol. 2007; 27:2493–2495. [PubMed: 17901372]

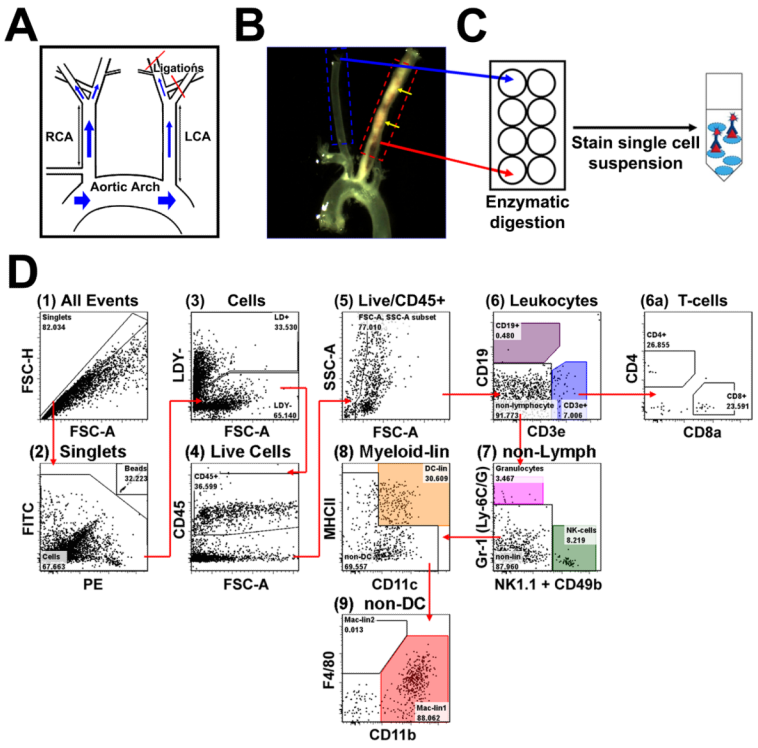

Figure 1. Development of a thirteen-parameter immunophenotyping study of leukocytes in the murine carotid artery

A, Disturbed flow was induced in the LCA of ApoE$^{-/-}$ mice by partial ligation surgery, while the contralateral RCA was used as an internal control. *B*, Ligated mice were fed a HFD for 4 to 28 days. Shown is a representative micrograph displaying diffuse atherosclerosis (yellow arrows) in LCA, but not in RCA, two weeks post-ligation. *C*, LCAs (dashed red box) and RCAs (dashed blue box in (B) obtained from 3 mice at a given time point were pooled (regarded as n=1) and vascular leukocytes extracted. *D*, Shows the gating strategy used for flow cytometry analyses for a representative arterial leukocyte sample harvested from LCA 7 days post-ligation. Ultra-bright counting beads (D2) were used to calculate absolute cell counts. Gate numbers indicate percent of parent. FSC-H, forward scatter height; FSC-A, forward scatter area; SSC-A, side scatter area.

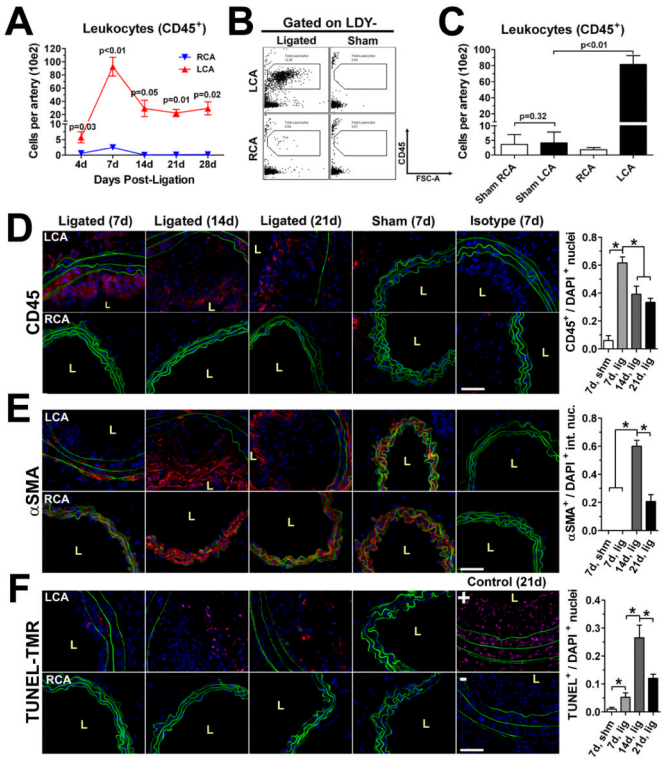

Figure 2. Dynamic infiltration of leukocytes into LCA in response to disturbed flow

A, Leukocyte ($CD45^+$) accumulation in mouse carotids was examined by the thirteen-parameter immunophenotyping analysis using LCA or RCA over a 4 week time course following ligation and HFD. Graph depicts number of cells (in hundreds) per carotid artery (n=4 to 5 pools of 3 arteries each). *B-C*, Leukocyte counts in LCA and RCA were compared by our flow cytometry method, using ligated and sham-operated mice (n=3 pools of 3 arteries each) at 7 days post-ligation. Shown are representative dot plots (B) and leukocyte numbers (C). *D-F*, Flow cytometry data were confirmed by immunofluorescence staining for CD45 (D), αSMA (E), or TUNEL stain (F) (red) in LCA and RCA frozen cross-sections obtained 7 (n=7), 14 (n=6), or 21 (n=7) days post-ligation along with 7 day sham-ligated controls (n=3), and isotype control stains. Elastic laminae autofluorescence (green) and nuclear staining by DAPI (blue) are shown. Quantitations of $CD45^+$, intimal αSMA^+, and $TUNEL^+$ staining nuclei residing in the arterial wall are shown to the right of their respective micrographs (D-F). Data are mean values ±SEM. p values in (A) denote comparisons of LCA versus RCA; in (D-F), magnification x40; scale bars, 50 μm; L, lumen; *, $p<0.05$.

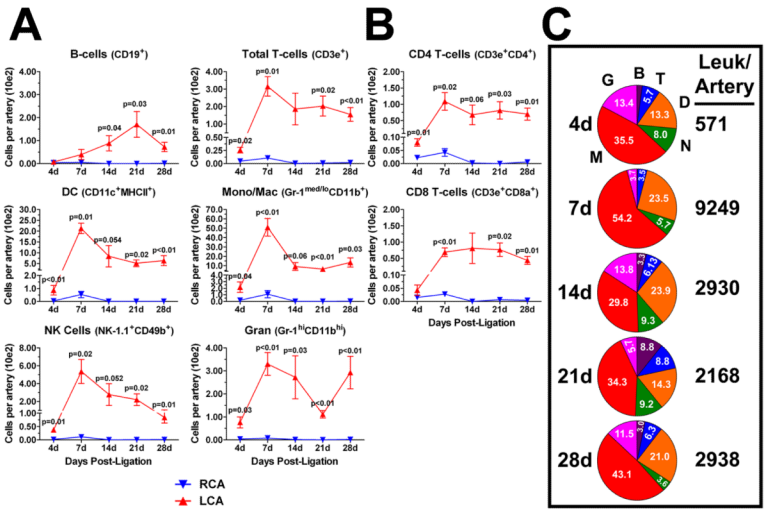

Figure 3. Disturbed flow induces a transient peak accumulation of innate cells, sustained T-cell accumulation, and delayed B-cell entry into LCA

The flow cytometry data shown in Figure 2a was further analyzed to quantitate dynamic changes in specific immune cell lineages. *A*, Leukocytes ($CD45^+$) were subdivided into six major immune cell types (B- and T-cells, DCs, monocyte/macrophage, NK cells and granulocytes) over a four week time course in LCA and RCA. *B*, T-cells were further subdivided into CD4 and CD8 T-cells. Shown (A-B) are absolute cell numbers (in hundreds) per carotid artery (n=4 to 5 pools of 3 arteries each). *C*, Pie charts show compositional analyses of vascular leukocytes in the flow-disturbed LCA, presented in (A). Each pie slice denotes mean percentage of total leukocytes (white numbers). Numbers to the right of the pie charts denote mean leukocyte numbers per carotid artery. Data are mean values ±SEM. B, B-cells; T, T-cells; D, DCs; N, NK-cells; M, macrophages; G, granulocytes.

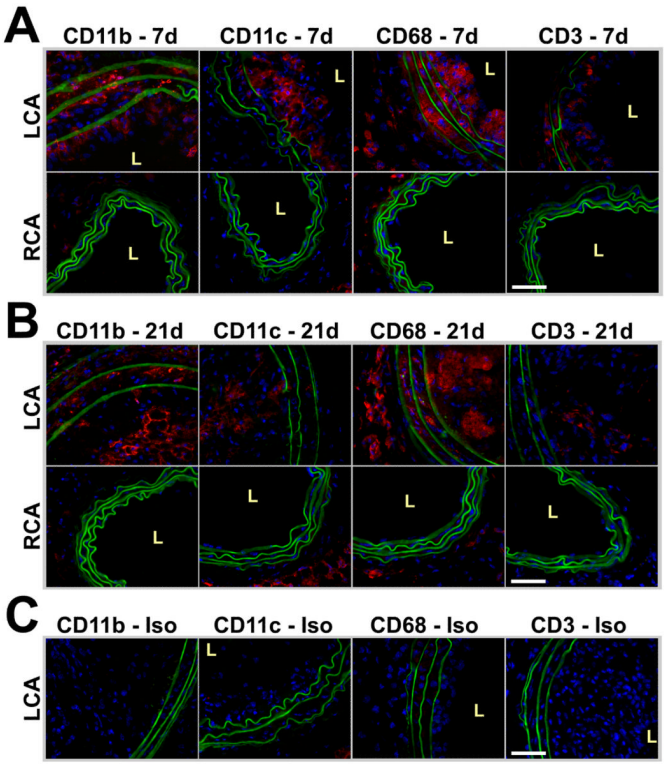

Figure 4. Disturbed flow induces accumulation of macrophages, dendritic cells (DC) and T-cells in LCA

A-B, Frozen sections from LCA and RCA obtained 7 (A) or 21 days (B) post-ligation were stained red with CD68, CD11b, CD11c, CD3, or isotype controls (C). Shown are representative images of n=7 (7d images) or n=5-7 (21d images). Elastic laminae autofluorescence (green) and nuclear staining by DAPI (blue) are shown. Magnification x40 (E); scale bars, 50 μm; L, lumen.

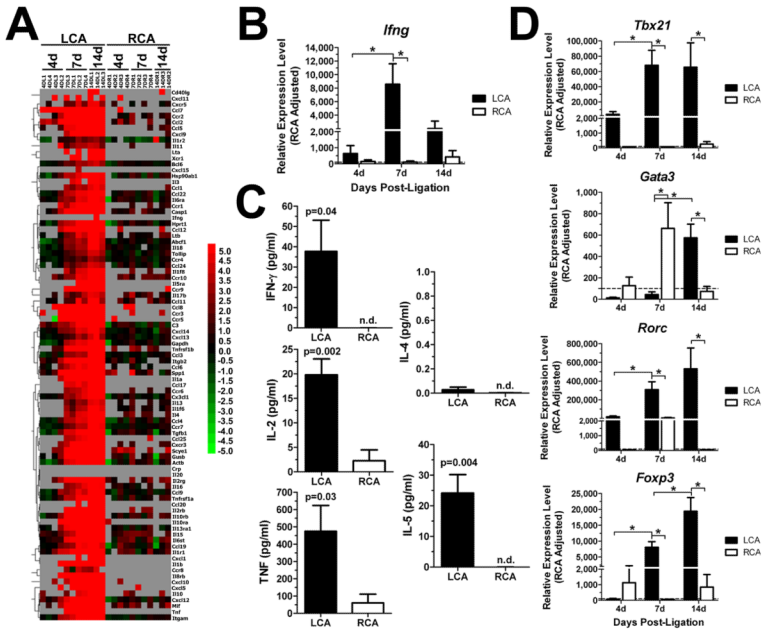

Figure 5. Dynamic changes in expression of cytokines and chemokines in LCA by disturbed flow

A-B, D, Total RNAs obtained from LCA and RCA were analyzed by PCR cytokine arrays (A) or by qPCR (B and D). The heat map shown in (A) displays relative expression levels of cytokines and cytokine receptors in LCA compared to RCA. Green indicates downregulation, black indicates no change, and red indicates upregulation. Grey boxes indicate undetectable copy number (>35 cycles). Additional qPCR was carried out using the total RNAs to determine expression of *Ifng* (B) and *Tbx21, Gata3, Rorc, Foxp3* (D). Shown are data for n=4 (4 and 7 day) and n=3 (14 day). *C*, Production of IFNγ, IL-2, TNFα, IL-4, and IL-5 proteins was determined by ELISA using 7 day post-ligation LCA and RCA stimulated ex vivo with TPA and ionomycin for 16 hr (n=5). Data are mean ±SEM. *, $p<0.05$. n.d., not detected.